Modeling of bending-torsion couplings in active-bending structures. Application to the design of elastic gridshell.

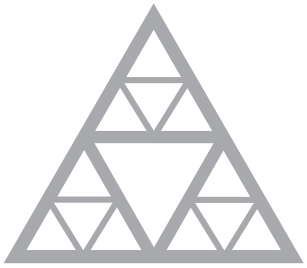

École des Ponts

ParisTech

Thèse n. xxxxx
présenté le 01 décembre 2017
à l'Ecole des Ponts ParisTech
laboratoire Navier
Université Paris-Est

pour l'obtention du grade de Docteur ès Sciences
par

Lionel du Peloux

acceptée sur proposition du jury:

Prof Name Surname, président du jury
Prof Name Surname, directeur de thèse
Prof Name Surname, rapporteur
Prof Name Surname, rapporteur
Prof Name Surname, rapporteur

Paris, Ecole des Ponts ParisTech, 2016

Contents

5 Elastic rod : equilibrium approach

5.1 Introduction

Ici on explique que l'approche par les équations d'équilibre est beaucoup plus directe que l'approche énergétique.

5.1.1 Goals and contribution

Dans ce chapitre, après un bref rappel sur le cadre mathématique d'étude des courbes paramétrique de l'espace, on présente les notions de courbures et de torsion géométrique associées au repère de fraient. On montre ensuite le cas plus général d'un repère mobile quelconque attaché à une courbe gamma. On définit enfin la particularité d'un repère mobile adapté à un courbe, et on présente, en sus du repère de Frenet, une approche différente pour accrocher des repères le long d'une courbe (Bishop / RMF / Zéro-twisting frame)

Ici il faudrait préciser la terminologie des auteurs / équations / hypothèses : Euler-Bernoulli, Navier-Bernoulli, Kirchhoff, Love, Clebesh, Cosserat, Vlassov

5.1.2 Related work

On peu s'instruire dans la publi de Dill [Dil92]. Regarder en particulier le premier chapitre de l'HDR de Neukirch [Neu09]. Regarder également la chronologie des modèles proposée dans la thèse de Theetten [The07]. Pourquoi pas proposer une frise chronologique + un tableau de synthèse des hyptohèses.

[Dil92] **(author?)** [Neu09] [ABW99] [Hoo06] [LL09] [Spi08] [Ant05]

[Neu09] : p69 - [Dil92] : p16

Dans les tentatives dans notre domaine, citer :

Départ : [Day65] : already includes a rotational DOF !! [Wak80] [Bar99] : revue intéressante de la DR.

3 pts classique : [ABW99] [DBC06]

2 x 3pts : [BAK13]

6 Dofs : [DKZ14]

4Dofs : [dPTL+15] [DZK16]

Dans le champ de l'animation avec élément finis [DLP13] [MPW14]

5.1.3 Overview

Résumé du chapitre

5.2 Dynamical equations for Kirchhoff rods

A thorough order-of-magnitude analysis is exposed in [Dil92, BEL+93]

A larger scope full development is given in [Ant05]

5.2.1 Assumptions

- axial extension is small
- sections remain planar in the deformed configuration
- sections remlain perpendicular to the centerline in the deformed configuration

ces équations sont valables à l'ordre 2 en α où :

$$\alpha = \max_{s\in[0,L]} \{|\kappa(s)|h, |\bar{\kappa}(s)|h, h/L\} \tag{5.1}$$

On fait par ailleurs l'hypothèse inextensible pour la dérivation du repère materiel.

dynamical equations

Writing the balance of linear and angular momentum of a beam slice of infinitesimal yields to the dynamic Kirchhoff equations for a slender beam. An extensive proof of this development is available in [Dil92].

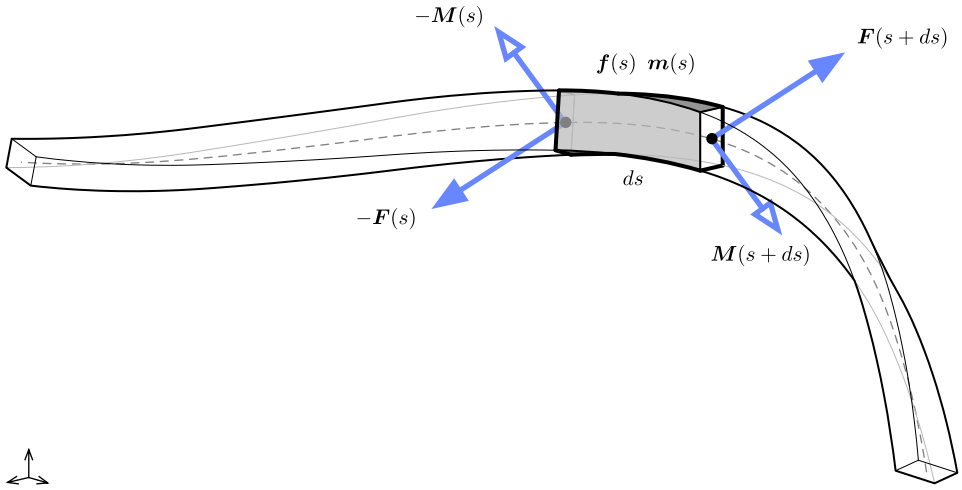

Figure 5.1 – Internal forces ($\boldsymbol{F}$) and moments ($\boldsymbol{M}$) acting on an infinitesimal beam slice of length ds. The beam is also subject to distributed external forces ($\boldsymbol{f}$) and moments ($\boldsymbol{m}$). By convention, internal forces and moments are forces and moments applied by the right part to the left part of the beam.

1 2 3

5.2.2 Balance of linear momentum

On fait un bilan sur une tranche d'épaisseur ds, de centre de gravité G positionné en $\boldsymbol{x}_G$:

$$\boldsymbol{F}(s+ds) - \boldsymbol{F}(s) + \boldsymbol{f}(s)ds = \left(\frac{\partial \boldsymbol{F}}{\partial s}(s) + \boldsymbol{f}(s)\right)ds = (\rho S ds)\ddot{\boldsymbol{x}}_G \tag{5.2}$$

Which leads to the first equation of Kirchhoff law :

$$\frac{\partial \boldsymbol{F}}{\partial s} + \boldsymbol{f} = \rho S \ddot{\boldsymbol{x}}_G \tag{5.3}$$

[1] "The principal normal, binormal, and torsion of the axis, viewed as an element of a space curve, have no special significance in the theory of rods. Use of those special directions as base vectors does not simplify the theory and can mislead the reader into attributing significance to them when none exists. In particular, the curvature of the rod should not be confused with the curvature of the space curve which the axis forms." [Dil92, p.5]

[2] "Kirchhoff's theory can only apply to that class of problems for three dimensional bodies such that the loads on the sides are relatively small and slowly varying. The dominate mode of deformation must be a global bending and twisting with small axial extension. If there are substantial local variations in curvatures or substantial transverse shears, his theory of bending of rods will not provide a satisfactory first approximation." [Dil92, p.18]

[3] "There are no constitutive relations for F_1 or F_2. They are determined by the balance of momentum as in the elementary linear theory of bending of rods." [Dil92, p.15]

5.2.3 Balance of angular momentum

On fait un bilan sur une tranche d'épaisseur ds, de centre de gravité G positionné en $\boldsymbol{x}_G$. On applique le théorème du moment cinétique dans un référentiel inertiel :

$$\begin{aligned}\frac{d}{dt}(dI_G) &= \boldsymbol{M}(s+ds) - \boldsymbol{M}(s) + \boldsymbol{m}(s)ds + (\tfrac{1}{2}ds\boldsymbol{x}') \times \boldsymbol{F}(s+ds) + (-\tfrac{1}{2}ds\boldsymbol{x}') \times -\boldsymbol{F}(s) \\ &= \left(\frac{\partial \boldsymbol{M}}{\partial s}(s) + \boldsymbol{m}(s) + \boldsymbol{x}' \times \boldsymbol{F}(s)\right) ds\end{aligned} \tag{5.4}$$

L'évolution temporelle des vecteurs matériels est cette fois décrite par un vecteur de Darboux temporel – spin vector in [BEL+93] – noté $\boldsymbol{\Lambda}$ tel que : Compatibility equation between the curvature vector and the spin vector ($\dot{\kappa \boldsymbol{b}} - \boldsymbol{\Lambda}' = \boldsymbol{\Lambda} \times \kappa \boldsymbol{b}$).

$$\dot{\boldsymbol{d}}_i(s) = \boldsymbol{\Lambda}(t) \times \boldsymbol{d}_i(s) \quad , \quad \boldsymbol{\Lambda}(t) = \begin{bmatrix} \Lambda_3(t) \\ \Lambda_1(t) \\ \Lambda_2(t) \end{bmatrix} \tag{5.5}$$

Les lois de composition / dérivation de la mécanique nous permettent décrire :

$$\frac{d}{dt}(dI_G) = dI_G \dot{\boldsymbol{\Lambda}} + \boldsymbol{\Lambda} \times dI_G \tag{5.6}$$

Qu'est ce qu'on met dans dI_G ? Et bien tout simplement l'opérateur d'inertie de la section, qui s'exprime à l'aide des moments quadratiques des directions principales de la façon suivante, dans la base des directions principales d'inertie au premier ordre en ds :

$$dI_G = \begin{bmatrix} dI_{G3} & 0 & 0 \\ 0 & dI_{G1} & 0 \\ 0 & 0 & dI_{G2} \end{bmatrix} \simeq \rho ds \begin{bmatrix} I_1 + I_2 & 0 & 0 \\ 0 & I_1 & 0 \\ 0 & 0 & I_2 \end{bmatrix} \tag{5.7}$$

Where :

$$dI_{G3} = \int_V \rho(x_1^2 + x_2^2)\, dV \simeq \rho ds \int_V (x_1^2 + x_2^2)\, dx_1 dx_2 \simeq \rho ds (I_1 + I_2) \tag{5.8a}$$

$$dI_{G1} = \int_V \rho(x_2^2 + x_3^2)\, dV \simeq \rho ds \int_V x_2^2\, dx_1 dx_2 \simeq \rho ds I_1 \tag{5.8b}$$

$$dI_{G2} = \int_V \rho(x_1^2 + x_3^2)\, dV \simeq \rho ds \int_V x_1^2\, dx_1 dx_2 \simeq \rho ds I_2 \tag{5.8c}$$

Et l'on peut alors écrire la seconde loi de Kirchhoff sous la forme suivante :

$$\frac{\partial \boldsymbol{M}}{\partial s}(s) + \boldsymbol{m}(s) + \boldsymbol{x}' \times \boldsymbol{F}(s) = \rho \begin{bmatrix} (I_1 + I_2)\dot{\Lambda}_3 + (I_2 - I_1)\Lambda_1\Lambda_2 \\ I_1(\dot{\Lambda}_1 + \Lambda_2\Lambda_3) \\ I_2(\dot{\Lambda}_2 - \Lambda_3\Lambda_1) \end{bmatrix} \tag{5.9}$$

On peut alors conclure sur l'expression de l'equation de kirchoff : [4,5]

$$\frac{\partial \boldsymbol{M}}{\partial s}(s) + \boldsymbol{m}(s) + \boldsymbol{d}_3 \times \boldsymbol{F}(s) = I_1 \boldsymbol{d}_1 \times \ddot{\boldsymbol{d}}_1 + I_2 \boldsymbol{d}_2 \times \ddot{\boldsymbol{d}}_2 \tag{5.10}$$

[4] Recall that : $\dot{\boldsymbol{d}}_i = \boldsymbol{\Lambda} \times \boldsymbol{d}_i$

[5] Remark that : $(\boldsymbol{\Lambda} \times \dot{\boldsymbol{d}}_i) \times \boldsymbol{d}_i = \Lambda_i(\boldsymbol{\Lambda} \times \dot{\boldsymbol{d}}_i)$

5.3 Equations of motion

5.3.1 Constitutive equations

"An order-of-magnitude analysis leading ..."

Attention, pas d'effort normal par loi constitutive en principe car on est dans un modèle inextensible. L'effort normal est calculé par la loi d'équilibre avec les moments et/ou efforts tranchants. Ici, on postulera tout de même une telle loi constitutive pour la résolution numérique. Ce qui nous amène à considérer une tige quasiment inextensible.

point à creuser. en gros je suis entrain de dire que dans le modèle classique à 3DOF type Douthe ou Barnes, il n'est pas nécessaire d'introduire la raideur axiale (mais alors où intervient la section ?). L'effort normal est déduit des équations d'équilibre.

En fait cela ne semble pas possible. Il faut alors revenir à l'équation constitutive qui donne l'effort normal, mais alors quid de l'hypothèse quasistatique ?

Dans le fond, l'hyptohèse d'inextensibilité c'est dire que les déformations axiales sont négligeable devant les autres modes de déformation (flexion et/ou torsion). Mais pour caractériser l'effort normal lui même, il faut bien considérer une élongation.

Ou alors, peut-être qu'il faut comprendre que l'effort normal est déduit uniquement des conditions aux limites et/ou éventuellement des efforts extérieurs appliqués à la centerline.

Pour comprendre le traitement de l'inextensibilité, regarder [Ant05] p50. Qu'apporte l'hypothèse d'inextensibilité. Est-elle raisonnable. Tps de calcul par rapport au cas extensible.

$$\boldsymbol{N} = ES\epsilon\boldsymbol{d}_3 \tag{5.11a}$$
$$\boldsymbol{M_1} = EI_1(\kappa_1 - \overline{\kappa_1})\boldsymbol{d}_1 \tag{5.11b}$$
$$\boldsymbol{M_2} = EI_2(\kappa_2 - \overline{\kappa_2})\boldsymbol{d}_2 \tag{5.11c}$$
$$\boldsymbol{Q} = [GJ(\theta' - \bar{\theta}') - EC_w(\theta''' - \bar{\theta}''')]\boldsymbol{d}_3 \tag{5.11d}$$

where :

$$I_1 = \int_S x_2^2 \, dx_1 dx_2 \tag{5.12}$$

$$I_2 = \int_S x_1^2 \, dx_1 dx_2 \tag{5.13}$$

$$J = \int_S (x_1^2 + x_2^2 + x_1 \frac{\partial \phi}{\partial x_2} - x_2 \frac{\partial \phi}{\partial x_1}) \, dx_1 dx_2 \tag{5.14}$$

with $\phi(x_1, x_2)$ is the warping function of the cross section.

5.3.2 Internal forces and moments

Efforts internes de coupure :

$$\boldsymbol{F}_{int} = N\boldsymbol{d}_3 + F_1\boldsymbol{d}_1 + F_2\boldsymbol{d}_2 \tag{5.15a}$$
$$\boldsymbol{M}_{int} = Q\boldsymbol{d}_3 + M_1\boldsymbol{d}_1 + M_2\boldsymbol{d}_2 \tag{5.15b}$$

Efforts externes appliqués linéiques :

$$\boldsymbol{f}_{ext} = f_3\boldsymbol{d}_3 + f_1\boldsymbol{d}_1 + f_2\boldsymbol{d}_2 \tag{5.16a}$$
$$\boldsymbol{m}_{ext} = m_3\boldsymbol{d}_3 + m_1\boldsymbol{d}_1 + m_2\boldsymbol{d}_2 \tag{5.16b}$$

5.3.3 Rod dynamic

First Kirchhoff law projecting on the material frame basis :

$$N' + \kappa_1 F_2 - \kappa_2 F_1 + f_3 = \rho S\ddot{x}_3 \tag{5.17a}$$
$$F_1' + \kappa_2 N - \tau F_2 + f_1 = \rho S\ddot{x}_1 \tag{5.17b}$$
$$F_2' - \kappa_1 N + \tau F_1 + f_2 = \rho S\ddot{x}_2 \tag{5.17c}$$

Qu'on écrit vectoriellement :

$$\boldsymbol{F}' + \boldsymbol{\Omega} \times \boldsymbol{F} + \boldsymbol{f}_{ext} = \rho S\ddot{\boldsymbol{x}} \quad with \quad \boldsymbol{F}' = \begin{bmatrix} F_1' & F_2' & N' \end{bmatrix}^T \tag{5.18}$$

This is nothing but the application of the transport theorem when differentiating a vector expressed in the material frame :

$$\left.\frac{\partial \boldsymbol{F}}{\partial s}\right|_{global} = \left.\frac{\partial \boldsymbol{F}}{\partial s}\right|_{local} + \boldsymbol{\Omega}(s) \times \boldsymbol{F} \tag{5.19}$$

Second Kirchhoff law projecting on the material frame basis : [6]

$$Q' + \kappa_1 M_2 - \kappa_2 M_1 + m_3 = (I_1 + I_2)\dot{\Lambda}_3 + (I_2 - I_1)\Lambda_1\Lambda_2 \tag{5.20a}$$
$$M_1' + \kappa_2 Q - \tau M_2 - F_2 + m_1 = I_1(\dot{\Lambda}_1 + \Lambda_2\Lambda_3) \tag{5.20b}$$
$$M_2' - \kappa_1 Q + \tau M_1 + F_1 + m_2 = I_2(\dot{\Lambda}_2 - \Lambda_3\Lambda_1) \tag{5.20c}$$

Qu'on écrit vectoriellement :

$$\boldsymbol{M}' + \boldsymbol{\Omega} \times \boldsymbol{M} + \boldsymbol{m}_{ext} + \boldsymbol{d}_3 \times \boldsymbol{F} = I_1\boldsymbol{d}_1 \times \ddot{\boldsymbol{d}}_1 + I_2\boldsymbol{d}_2 \times \ddot{\boldsymbol{d}}_2 \tag{5.21}$$
$$with \quad \boldsymbol{M}' = \begin{bmatrix} M_1' & M_2' & Q' \end{bmatrix}^T \tag{5.22}$$

[6] As explained in [Dil92, p. 18], if the inextensibility assumption does not hold, the right terms to consider are $-(1+\epsilon)F_2$ in eq. (5.20b) and $(1+\epsilon)F_1$ in eq. (5.20c).

This is nothing but the application of the transport theorem when differentiating a vector expressed in the material frame :

$$\left.\frac{\partial \boldsymbol{M}}{\partial s}\right|_{global} = \left.\frac{\partial \boldsymbol{M}}{\partial s}\right|_{local} + \boldsymbol{\Omega}(s) \times \boldsymbol{M} \tag{5.23}$$

5.4 Geometric interpretation

Ici, on peut mettre l'interprétation géométrique (cf pdf LDP notes). Cela consiste essentiellement à 2/3 schémas bien pensés à produire + à écrire les projections au 1er ordre.

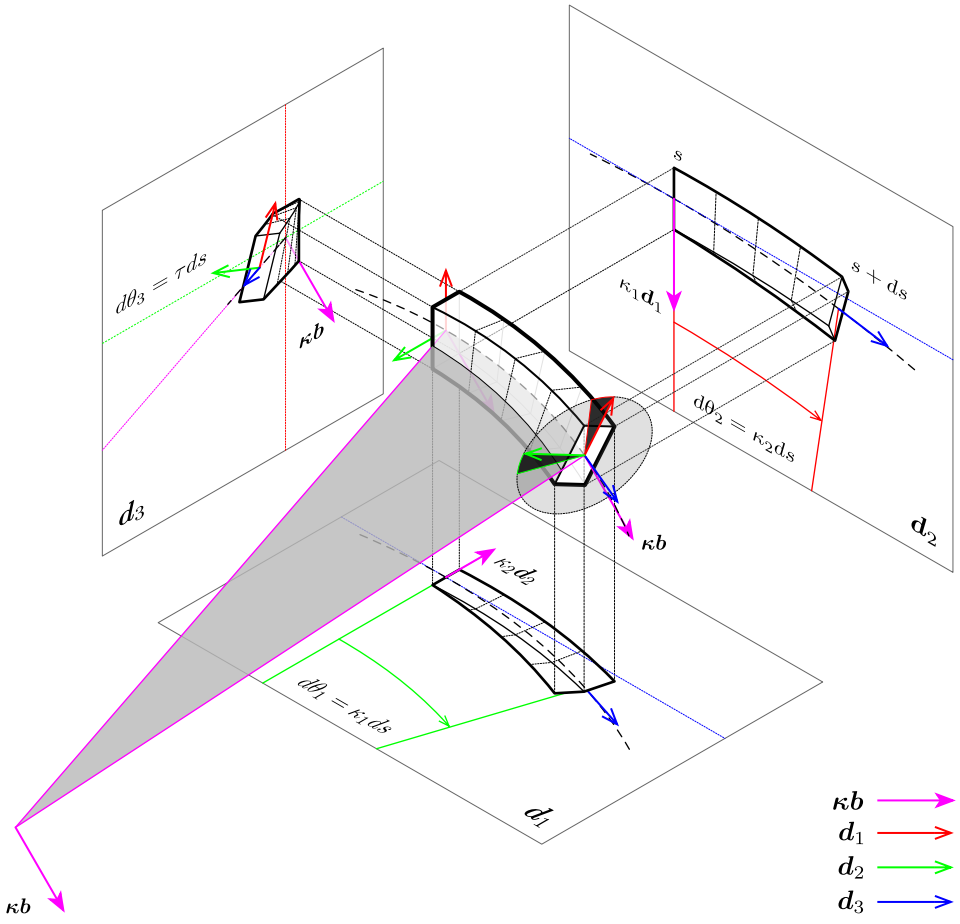

Figure 5.2 – Osculating circles for a spiral curve at different parameters.

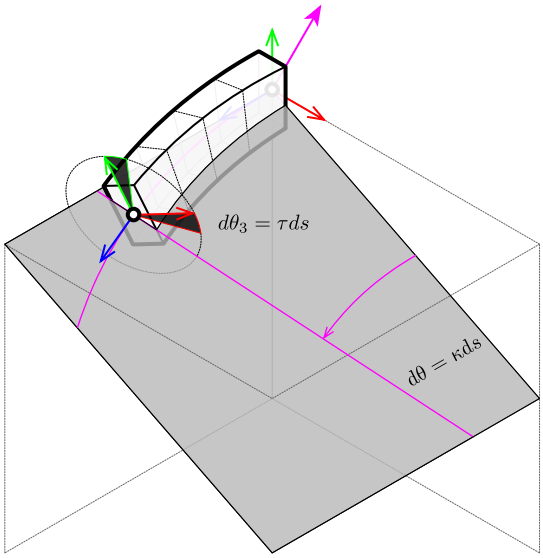

(a) Infinitesimal deformation.

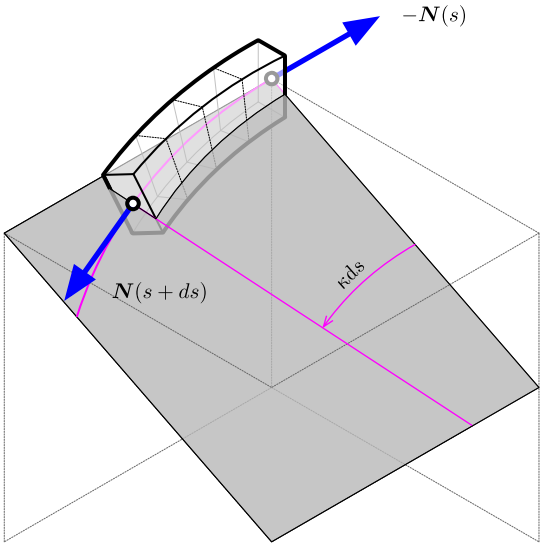

(b) Contributions of the internal forces.

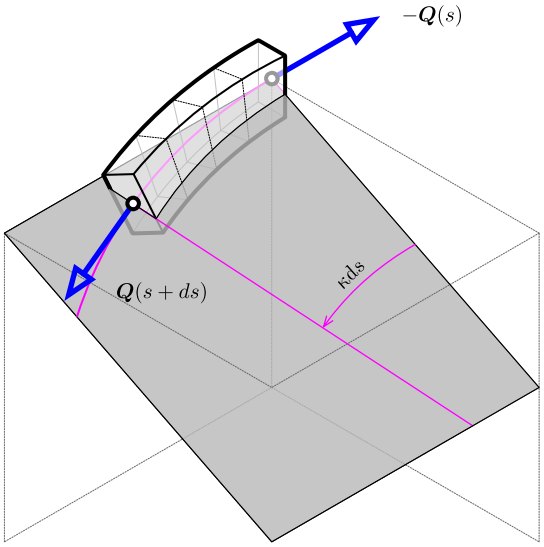

(c) Contributions of the internal moments.

Figure 5.3 – Influence of the centerline curvature (κ) in the deviation of internal forces and moments along the centerline.

Contributions to the balance of forces

$\boldsymbol{N}(s+ds)$ is deviated from $\boldsymbol{d}_3(s)$ by an angle $d\theta = \kappa ds$ along ds (fig. 5.3b). Thus, its overall contribution to the balance of forces over $\boldsymbol{d}_3(s)$ is :

$$N(s+ds)\cos(\kappa ds) - N(s) = N'(s)ds + o(ds)$$

Contributions to the balance of moments

$\boldsymbol{Q}(s+ds)$ is deviated from $\boldsymbol{d}_3(s)$ by an angle $d\theta = \kappa ds$ along ds (fig. 5.3c). Thus, its overall contribution to the balance of moments over $\boldsymbol{d}_3(s)$ is :

$$Q(s+ds)\cos(\kappa ds) - Q(s) = Q'(s)ds + o(ds)$$

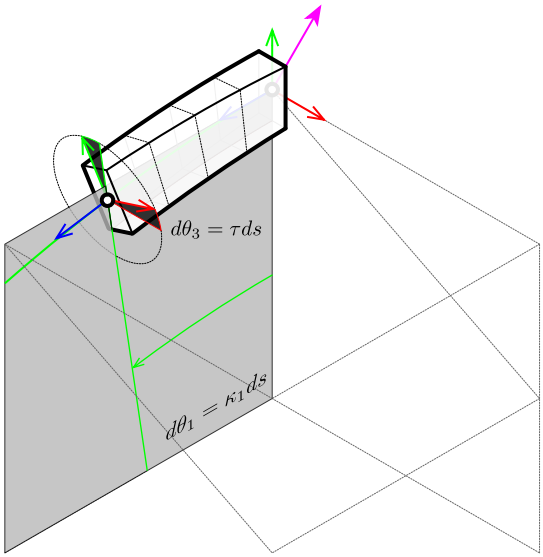

(a) Infinitesimal deformation.

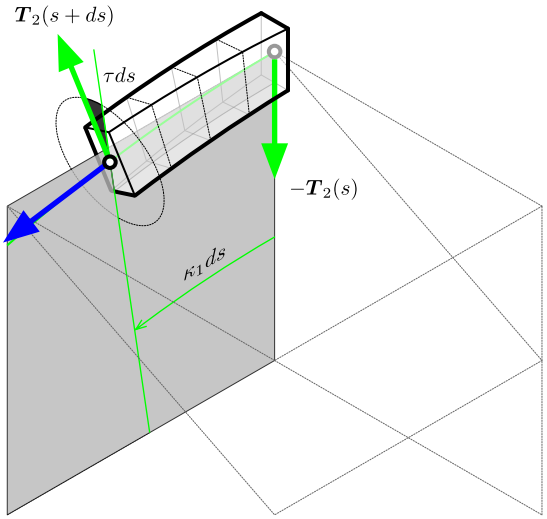

(b) Contributions of the internal forces.

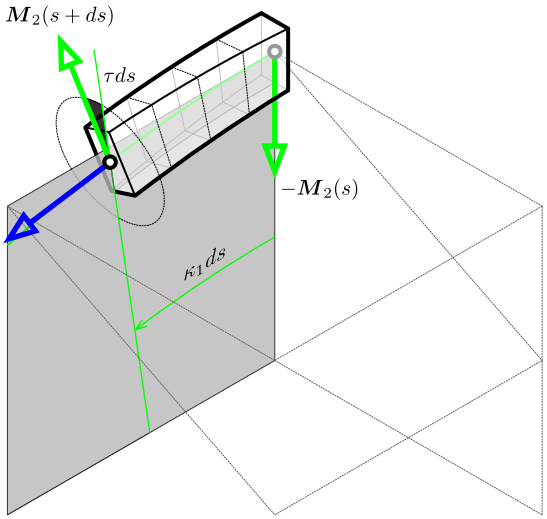

(c) Contributions of the internal moments.

Figure 5.4 – Influence of the first material curvature (κ_1) in the deviation of internal forces and moments along the centerline.

Contributions to the balance of forces

$\boldsymbol{T}_2(s+ds)$ is deviated from $\boldsymbol{d}_2(s)$ by the combined angles $d\theta_3 = \tau ds$ and $d\theta_2 = \kappa_2 ds$ along ds (fig. 5.4b). Thus, its overall contribution to the balance of forces over $\boldsymbol{d}_1(s)$ is :

$$-T_2(s+ds)\sin(\tau ds)\cos(\kappa_2 ds) = -\tau T_2(s)ds + o(ds)$$

$\boldsymbol{T}_2(s+ds)$ is deviated from $\boldsymbol{d}_2(s)$ by the combined angles $d\theta_3 = \tau ds$ and $d\theta_1 = \kappa_1 ds$ along ds (fig. 5.4b). Thus, its overall contribution to the balance of forces over $\boldsymbol{d}_2(s)$ is :

$$-T_2(s) + T_2(s+ds)\cos(\tau ds)\cos(\kappa_1 ds) = T_2'(s)ds + o(ds)$$

$\boldsymbol{T}_2(s+ds)$ is deviated from $\boldsymbol{d}_2(s)$ by the combined angles $d\theta_3 = \tau ds$ and $d\theta_1 = \kappa_1 ds$ along ds (fig. 5.4b). Thus, its overall contribution to the balance of forces over $\boldsymbol{d}_3(s)$ is :

$$T_2(s+ds)\cos(\tau ds)\sin(\kappa_1 ds) = \kappa_1 T_2(s)ds + o(ds)$$

$\boldsymbol{N}(s+ds)$ is deviated from $\boldsymbol{d}_3(s)$ by the combined angles $d\theta_2 = \kappa_2 ds$ and $d\theta_1 = \kappa_1 ds$ along ds (fig. 5.4b). Thus, its overall contribution to the balance of forces over $\boldsymbol{d}_2(s)$ is :

$$-N(s+ds)\cos(\kappa_2 ds)\sin(\kappa_1 ds) = -\kappa_1 N(s)ds + o(ds)$$

Contributions to the balance of moments

$\boldsymbol{T}_2(s+ds)$ is deviated from the plane normal to $\boldsymbol{d}_1(s)$ by the angle $d\theta_3 = \tau ds$ along ds (fig. 5.4b). It produces a moment around $\boldsymbol{d}_1$ with the lever arm $b = \cos(\kappa_2 ds)ds$. Thus, its overall contribution to the balance of moments over $\boldsymbol{d}_1(s)$ is :

$$-T_2(s+ds)\cos(\tau ds)(\cos(\kappa_2 ds)ds) = -T_2(s)ds + o(ds)$$

$\boldsymbol{M}_2(s+ds)$ is deviated from $\boldsymbol{d}_2(s)$ by the combined angles $d\theta_3 = \tau ds$ and $d\theta_2 = \kappa_2 ds$ along ds (fig. 5.4c). Thus, its overall contribution to the balance of moments over $\boldsymbol{d}_1(s)$ is :

$$-M_2(s+ds)\sin(\tau ds)\cos(\kappa_2 ds) = -\tau M_2(s)ds + o(ds)$$

$\boldsymbol{M}_2(s+ds)$ is deviated from $\boldsymbol{d}_2(s)$ by the combined angles $d\theta_3 = \tau ds$ and $d\theta_1 = \kappa_1 ds$ along ds (fig. 5.4c). Thus, its overall contribution to the balance of moments over $\boldsymbol{d}_2(s)$ is :

$$-M_2(s) + M_2(s+ds)\cos(\tau ds)\cos(\kappa_1 ds) = M_2'(s)ds + o(ds)$$

$\boldsymbol{M}_2(s+ds)$ is deviated from $\boldsymbol{d}_2(s)$ by the combined angles $d\theta_3 = \tau ds$ and $d\theta_1 = \kappa_1 ds$ along ds (fig. 5.4c). Thus, its overall contribution to the balance of moments over $\boldsymbol{d}_3(s)$ is :

$$M_2(s+ds)\cos(\tau ds)\sin(\kappa_1 ds) = \kappa_1 M_2(s)ds + o(ds)$$

$\boldsymbol{Q}(s+ds)$ is deviated from $\boldsymbol{d}_3(s)$ by the combined angles $d\theta_2 = \kappa_2 ds$ and $d\theta_1 = \kappa_1 ds$ along ds (fig. 5.4c). Thus, its overall contribution to the balance of moments over $\boldsymbol{d}_2(s)$ is :

$$-Q(s+ds)\cos(\kappa_2 ds)\sin(\kappa_1 ds) = -\kappa_1 Q(s)ds + o(ds)$$

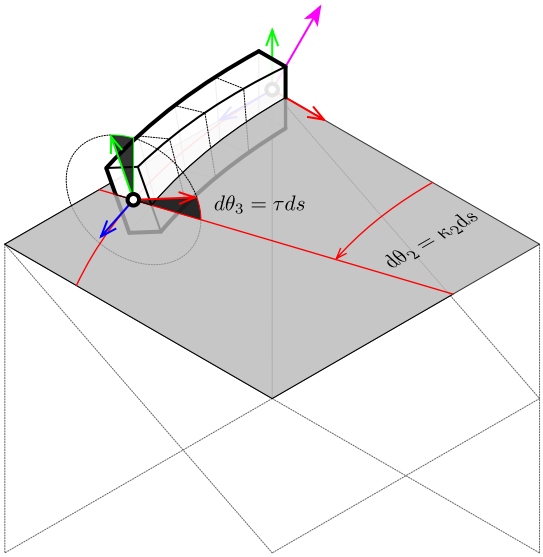

(a) Infinitesimal deformation.

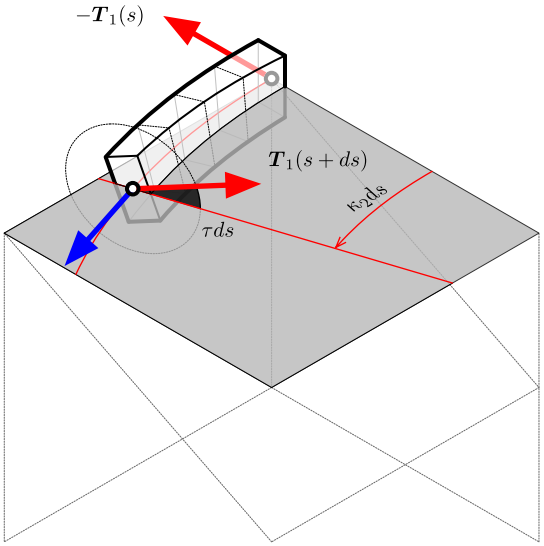

(b) Contributions of the internal forces.

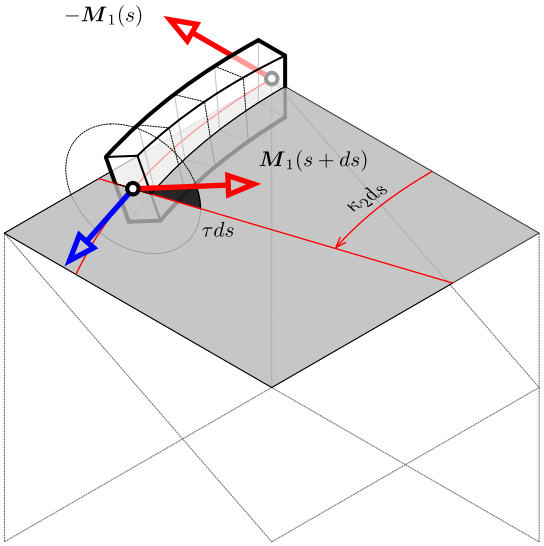

(c) Contributions of the internal moments.

Figure 5.5 – Influence of the second material curvature (κ_2) in the deviation of internal forces and moments along the centerline.

Contributions to the balance of forces

$\boldsymbol{T}_1(s+ds)$ is deviated from $\boldsymbol{d}_1(s)$ by the combined angles $d\theta_3 = \tau ds$ and $d\theta_2 = \kappa_2 ds$ along ds (fig. 5.5b). Thus, its overall contribution to the balance of forces over $\boldsymbol{d}_1(s)$ is :

$$-T_1(s) + T_1(s+ds)\cos(\tau ds)\cos(\kappa_2 ds) = T_1'(s)ds + o(ds)$$

$\boldsymbol{T}_1(s+ds)$ is deviated from $\boldsymbol{d}_1(s)$ by the combined angles $d\theta_3 = \tau ds$ and $d\theta_1 = \kappa_1 ds$ along ds (fig. 5.5b). Thus, its overall contribution to the balance of forces over $\boldsymbol{d}_2(s)$ is :

$$T_1(s+ds)\sin(\tau ds)\cos(\kappa_1 ds) = \tau T_1(s)ds + o(ds)$$

$\boldsymbol{T}_1(s+ds)$ is deviated from $\boldsymbol{d}_1(s)$ by the combined angles $d\theta_3 = \tau ds$ and $d\theta_2 = \kappa_2 ds$ along ds (fig. 5.5b). Thus, its overall contribution to the balance of forces over $\boldsymbol{d}_3(s)$ is :

$$-T_1(s+ds)\cos(\tau ds)\sin(\kappa_2 ds) = -\kappa_2 T_1(s)ds + o(ds)$$

$\boldsymbol{N}(s+ds)$ is deviated from $\boldsymbol{d}_3(s)$ by the combined angles $d\theta_1 = \kappa_1 ds$ and $d\theta_2 = \kappa_2 ds$ along ds (fig. 5.5b). Thus, its overall contribution to the balance of forces over $\boldsymbol{d}_1(s)$ is :

$$N(s+ds)\cos(\kappa_1 ds)\sin(\kappa_2 ds) = \kappa_2 N(s)ds + o(ds)$$

Contributions to the balance of moments

$\boldsymbol{T}_1(s+ds)$ is deviated from the plane normal to $\boldsymbol{d}_2(s)$ by the angle $d\theta_3 = \tau ds$ along ds (fig. 5.5b). It produces a moment around $\boldsymbol{d}_2$ with the lever arm $b = \cos(\kappa_1 ds)ds$. Thus, its overall contribution to the balance of moments over $\boldsymbol{d}_2(s)$ is :

$$T_1(s+ds)\cos(\tau ds)(\cos(\kappa_1 ds)ds) = T_1(s)ds + o(ds)$$

$\boldsymbol{M}_1(s+ds)$ is deviated from $\boldsymbol{d}_1(s)$ by the combined angles $d\theta_3 = \tau ds$ and $d\theta_2 = \kappa_2 ds$ along ds (fig. 5.5c). Thus, its overall contribution to the balance of moments over $\boldsymbol{d}_1(s)$ is :

$$-M_1(s) + M_1(s+ds)\cos(\tau ds)\cos(\kappa_2 ds) = M_1'(s)ds + o(ds)$$

$\boldsymbol{M}_1(s+ds)$ is deviated from $\boldsymbol{d}_1(s)$ by the combined angles $d\theta_3 = \tau ds$ and $d\theta_2 = \kappa_2 ds$ along ds (fig. 5.5c). Thus, its overall contribution to the balance of moments over $\boldsymbol{d}_2(s)$ is :

$$M_1(s+ds)\sin(\tau ds)\cos(\kappa_2 ds) = \tau M_1(s)ds + o(ds)$$

$\boldsymbol{M}_1(s+ds)$ is deviated from $\boldsymbol{d}_1(s)$ by the combined angles $d\theta_3 = \tau ds$ and $d\theta_2 = \kappa_2 ds$ along ds (fig. 5.5c). Thus, its overall contribution to the balance of moments over $\boldsymbol{d}_3(s)$ is :

$$-M_1(s+ds)\cos(\tau ds)\sin(\kappa_2 ds) = -\kappa_2 M_1(s)ds + o(ds)$$

$\boldsymbol{Q}(s+ds)$ is deviated from $\boldsymbol{d}_3(s)$ by the combined angles $d\theta_1 = \kappa_1 ds$ and $d\theta_2 = \kappa_2 ds$ along ds (fig. 5.5c). Thus, its overall contribution to the balance of moments over $\boldsymbol{d}_1(s)$ is :

$$Q(s+ds)\cos(\kappa_1 ds)\sin(\kappa_2 ds) = \kappa_2 Q(s)ds + o(ds)$$

5.5 Numerical resolution

5.5.1 Main hypothesis

On néglige les forces d'inertie liées à la rotation de l'élément (devant quoi ?? traitement quasi-statique par rapport à la rotation). Cette hypothèse est faite explicitement chez Florence Bertail :

"neglecting inertial momentum due to the vanishing cross-section lead to the following dynamic equations for a Kirchhoff rod" [CBd13]

> It follows that ω_1 and ω_2 can be neglected in the kinetic energy [...]. However, ω_3, which provides the angular momentum about the axis of the rod, must be retained, This assumption of Kirchhoff is consistent with the technical theory of beams where rotary inertia is known to provide corrections to the natural frequencies of vibration of $O(\alpha^2)$ if the length measure is the half-wave length. [Dil92, p. 17]

Cette hypothèse est faite mais passée sous silence chez Douthe, Adriaenssen, D'Amico lorsqu'ils déduisent l'effort tranchant du moment de flexion.

Principe :

- les équations constitutives permettent le calcul de M_1, M_2, Q à partir de la géométrie $\{\boldsymbol{x}, \theta\}$.

- La seconde loi de kirchhoff projetée sur les axes matériels 1 et 2 de la section me donnent accès aux efforts tranchants T_1 et T_2.

- La seconde loi de kirchhoff projetée sur les axes matériel 3 (tangente à la centerline) de la section me donnent l"hypothèse quasi-statique de Audoly.

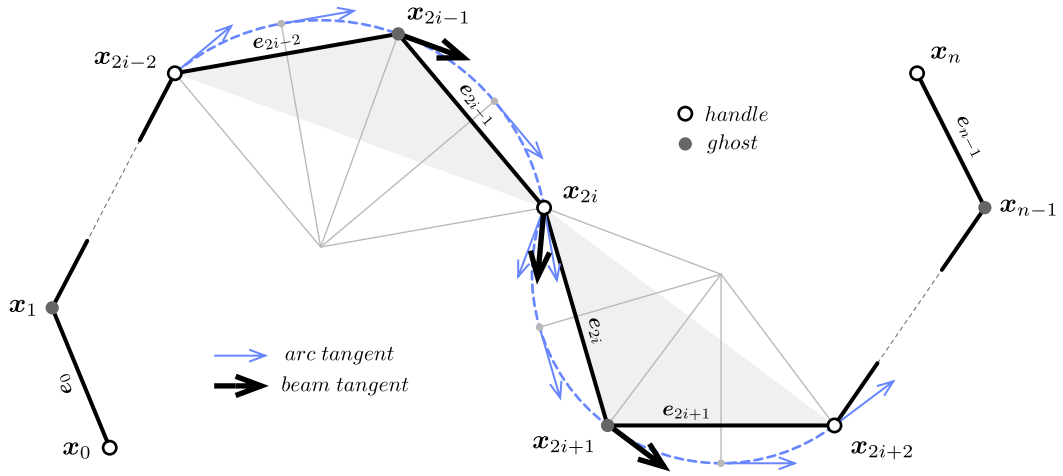

(a) Biarc model discrete centerline.

		open	closed
segments	n_s	n_s	n_s
edges	n_e	$2n_s$	$2n_s$
vertices	n	$2n_s + 1$	$2n_s$
ghosts	n_g	n_s	n_s
handles	n_h	$n_s + 1$	n_s

(b) Number of segments, edges and vertices whether the centerline is closed or open.

Figure 5.6 – Biarc model for a discrete beam. The centerline is divided into curved segments (grey solid hatch). Each segment is defined as a 3-noded element with uniform material and section properties. It has two end vertices (white) called *handle* as they are used to interact with the model, for instance to apply loads or restrains. It has one mid vertex (grey) called *ghost* as it is used only to enrich the segment kinematics and is not accessible to the end user.

5.5.2 Discret beam model

Let's introduce the discrete biarc model to describe the configuration of a beam. It is composed of a discrete curve called *centerline* and a discrete adapted frame called *material frame* as its axes are chosen to be the principal axes of the beam cross section (fig. 5.6a). The centerline itself is organized in n_s consecutive adjacent segments which are three-vertices and two-edges elements with uniform material and section properties.

Beams can either be closed or open. The corresponding number of vertices, edges and segments are reported in fig. 5.6b :

Centerline

The discrete centerline is a polygonal space curve (fig. 5.6a) defined as an ordered sequence of $n+1$ pairwise disjoint *vertices* : $\Gamma = (\boldsymbol{x}_0, \boldsymbol{x}_1, \dots, \boldsymbol{x}_n) \in \mathbb{R}^{3(n+1)}$. Consecutive pairs of vertices define n straight segments $(\boldsymbol{e}_0, \boldsymbol{e}_1, \dots, \boldsymbol{e}_{n-1})$ called *edges* and pointing from one vertex to the next one : $\boldsymbol{e}_i = \boldsymbol{x}_{i+1} - \boldsymbol{x}_i$:

$$\begin{cases} \boldsymbol{e}_i = \boldsymbol{x}_{i+1} - \boldsymbol{x}_i \\ l_i = \|\boldsymbol{e}_i\| \\ \boldsymbol{u}_i = \boldsymbol{e}_i / l_i \end{cases} \tag{5.24}$$

The length of the ith edge is denoted l_i and its unit director is denoted $\boldsymbol{u}_i$. The arc length of the ith vertex is denoted s_i and is given by :

$$\begin{cases} s_0 = 0 & i = 0 \\ s_i = \displaystyle\sum_{k=0}^{i-1} l_k & i \in [\![1, n-1]\!] \\ s_n = L & i = n \end{cases} \tag{5.25}$$

Thus, the centerline is parametrized by arc length and $\Gamma(s_i) = \boldsymbol{x}_i$. Additionally, we define the vertex-based mean length at vertex $\boldsymbol{x}_i$:

$$\begin{cases} \overline{l_0} = \frac{1}{2} l_0 & i = 0 \\ \overline{l_i} = \frac{1}{2}(l_{i-1} + l_i) & i \in [\![1, n-1]\!] \\ \overline{l_n} = \frac{1}{2} l_{n-1} & i = n \end{cases} \tag{5.26}$$

Segments

The discrete centerline is divided into n_s curved segments. Each segment is a three-noded element – see fig. 5.6a where the area covered by a segment is represented as a grey solid hatch. The ith segment is composed of three vertices $(\boldsymbol{x}_{2i}, \boldsymbol{x}_{2i+1}, \boldsymbol{x}_{2i+2})$ spanning two edges $(\boldsymbol{e}_{2i}, \boldsymbol{e}_{2i+1})$. The (i-1)th segment and the ith segment share the same vertex $\boldsymbol{x}_{2i}$ at arc length s_{2i}.

Each segment has two end vertices called *handle* ($\boldsymbol{x}_{2i}, \boldsymbol{x}_{2i+2}$) and one mid vertex called *ghost* ($\boldsymbol{x}_{2i+1}$) as this one is not accessible to the end user in order to interact with the model (link, restrain, loading, ...). Ghost vertices are used only for internal purpose to give a higher richness in the kinematic description of a segment than a two-noded segment would.

We define the *chord length* of the ith segment as the distance between $\boldsymbol{x}_{2i}$ and $\boldsymbol{x}_{2i+2}$: $L_i = \|\boldsymbol{e}_{2i} + \boldsymbol{e}_{2i+1}\|$.

Material and section properties

In addition, the model assumes that a segment has uniform section (S, I_1, I_2, J)[7] and material (E, G)[8] properties over its length : $s \in]s_{2i}, s_{2i+2}[$. For the sake of simplicity, we introduce for further calculations the *material stiffness matrix* ($\boldsymbol{B}_i$) attached to each segment. It has the following form in the material frame basis :

$$\boldsymbol{B}_i = \begin{bmatrix} EI_1 & 0 & 0 \\ 0 & EI_2 & 0 \\ 0 & 0 & GJ \end{bmatrix}_i \tag{5.27}$$

External loads

Also, the model assumes that each segment can be loaded with uniform external distributed forces ($\boldsymbol{f}_{ext}$) and moments ($\boldsymbol{m}_{ext}$).

External loads

External concentrated forces ($\boldsymbol{F}_{ext}$) and moments ($\boldsymbol{M}_{ext}$) are applied to the segment end vertices ($\boldsymbol{x}_{2i}$, $\boldsymbol{x}_{2i+2}$).

This discret model involves that axial, bending and torsion strains, section and material properties will be continuous fonctions of the arc length over each segment $]\boldsymbol{x}_{2i}, \boldsymbol{x}_{2i+2}[$. Discontinuities in strains, internal and external forces, internal and external moments will be located at handle vertices. The left and right limits of this fonctions at handle vertices will be denoted respectively by f^- and f^+. Possibly they are continuous at handle nodes that is the left and right limits agree ($f^- = f^+$).

Lets call : $l_i = \|\boldsymbol{e}_i\|$ with $i \in [0, n_e]$. Lets call : $u_i = \frac{\boldsymbol{e}_i}{l_i}$ with $i \in [0, n_e]$.

Lets call : $L_i = \|\boldsymbol{e}_{2i} + \boldsymbol{e}_{2i+1}\|$ with $i \in [0, n_g]$.

We have : $\boldsymbol{d}_{3,i+1/2} = \boldsymbol{u}_i$

Let $\boldsymbol{B}_i$ be the material stiffness matrix along the principal axes of inertia, uniform over

[7] S is the cross section area ; I_1, I_2 and J are the cross section principal moments of inertia.
[8] E is the elastic modulus and G is the shear modulus for the considered material

the slice $]\boldsymbol{x}_{2i}, \boldsymbol{x}_{2i+2}[$. Thus, it has the following form in the material basis :

$$\boldsymbol{B}_i = \begin{bmatrix} EI_1 & 0 & 0 \\ 0 & EI_2 & 0 \\ 0 & 0 & GJ \end{bmatrix}_i \tag{5.28}$$

Thus, one will write the constitutive equations for the bending moment in matrix notation as :

$$\boldsymbol{M}_i = \boldsymbol{B}_i(\boldsymbol{\kappa b}_i - \overline{\boldsymbol{\kappa b}}_i) \tag{5.29}$$

With $\boldsymbol{\kappa b} = \begin{bmatrix} \kappa_1 & \kappa_2 & \tau \end{bmatrix}^T$ expressed in the material frame.

5.5.3 Discret bending moments and curvatures

We assume that the internal bending moment and curvature are quadratic functions of the arc length over $]\boldsymbol{x}_{2i}, \boldsymbol{x}_{2i+2}[$. While they must be continuous over this interval, they might be discontinuous at handle vertices and be subjected to jump discontinuities in direction and magnitude.

Curvature at ghost vertices

For a given geometry of the centerline, the curvature binormal vector at ghost vertex $\boldsymbol{x}_{2i-1}$ (resp. $\boldsymbol{x}_{2i+1}$) is computed considering the circumscribed osculating circle passing through the vertices $(\boldsymbol{x}_{2i-2}, \boldsymbol{x}_{2i-1}, \boldsymbol{x}_{2i})$ of the $(i-1)th$ segment – resp. through the vertices $(\boldsymbol{x}_{2i}, \boldsymbol{x}_{2i+1}, \boldsymbol{x}_{2i+2})$ of the i-th segment.

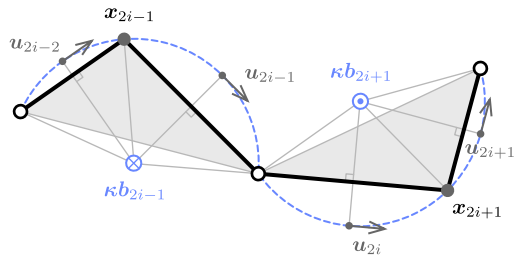

$$\kappa\boldsymbol{b}_{2i-1} = \frac{2}{L_{i-1}}\boldsymbol{u}_{2i-2} \times \boldsymbol{u}_{2i-1}$$

$$\kappa\boldsymbol{b}_{2i+1} = \frac{2}{L_i}\boldsymbol{u}_{2i} \times \boldsymbol{u}_{2i+1}$$

Unit tangent vectors at ghost vertices

This definition of the curvature leads to a natural definition of the unit tangent vector at ghost vertex $\boldsymbol{x}_{2i-1}$ (resp. $\boldsymbol{x}_{2i+1}$), as the unit vector tangent to the osculating circle of the $(i-1)th$ segment (resp. i-th segment) at that point.

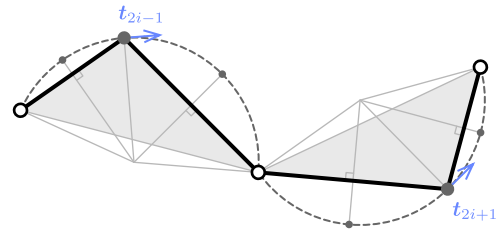

$$\boldsymbol{t}_{2i-1} = \frac{l_{2i-1}}{L_{i-1}}\boldsymbol{u}_{2i-2} + \frac{l_{2i-2}}{L_{i-1}}\boldsymbol{u}_{2i-1}$$

$$\boldsymbol{t}_{2i+1} = \frac{l_{2i+1}}{L_i}\boldsymbol{u}_{2i} + \frac{l_{2i}}{L_i}\boldsymbol{u}_{2i+1}$$

Left/right unit tangent vectors at handle vertices

Equivalently, the definition of the osculating circles of the $(i-1)th$ and i-th segments leads to a natural definition of the left $(\boldsymbol{t}^-_{2i})$ and right $(\boldsymbol{t}^+_{2i})$ unit tangent vectors at handle vertex $\boldsymbol{x}_{2i}$, for segments of uniform curvature. When both segments have the same curvature, left and right vectors agree.

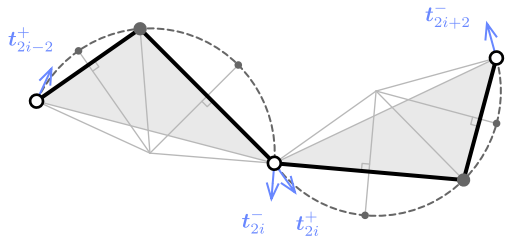

$$\boldsymbol{t}^-_{2i} = 2(\boldsymbol{t}_{2i-1} \cdot \boldsymbol{u}_{2i-1})\boldsymbol{u}_{2i-1} - \boldsymbol{t}_{2i-1}$$

$$\boldsymbol{t}^+_{2i} = 2(\boldsymbol{t}_{2i+1} \cdot \boldsymbol{u}_{2i})\boldsymbol{u}_{2i} - \boldsymbol{t}_{2i+1}$$

Unit tangent vectors at handle vertices

The unit tangent vector $\boldsymbol{t}_{2i}$ – that is the beam section normal – at handle vertex $\boldsymbol{x}_{2i}$ is chosen to be the mean of the left and right unit tangent vectors at that vertex.[9]

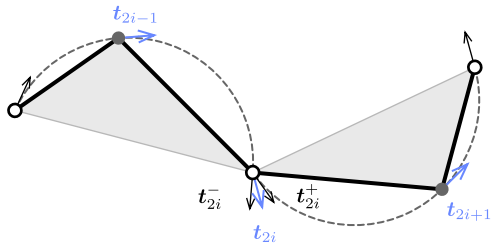

$$\boldsymbol{t}_{2i} = \frac{\boldsymbol{t}_{2i}^- + \boldsymbol{t}_{2i}^+}{\|\boldsymbol{t}_{2i}^- + \boldsymbol{t}_{2i}^+\|}$$

This way, the determination of the tangent vectors – or equivalently the section normals – in the static equilibrium configuration will be done in the flow of the dynamic relaxation process, without the need of introducing any additional degrees of freedom (for instance the usual Euler angles). The position of the vertices rules the orientation of the section normals.

Left/right bending moments at handle vertices

Given the unit tangent vector $\boldsymbol{t}_{2i}$, one can define the left ($\boldsymbol{\kappa}_{2i}^-$) and right ($\boldsymbol{\kappa}_{2i}^+$) curvatures at handle vertex $\boldsymbol{x}_{2i}$. The left curvature is initially evaluated from the left osculating circle, defined as the circle passing through $\boldsymbol{x}_{2i-1}$ and $\boldsymbol{x}_{2i}$ and tangent to $\boldsymbol{t}_{2i}$ at $\boldsymbol{x}_{2i}$. The right curvature is initially evaluated from the right osculating circle, defined as the circle passing through $\boldsymbol{x}_{2i}$ and $\boldsymbol{x}_{2i+1}$ and tangent to $\boldsymbol{t}_{2i}$ at $\boldsymbol{x}_{2i}$.[10,11]

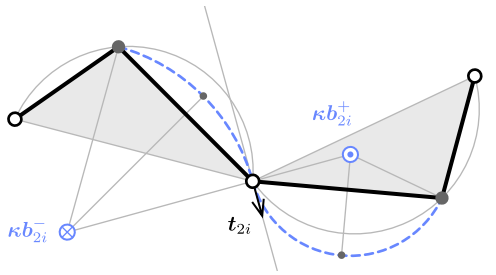

$$\boldsymbol{\kappa b}_{2i}^- = \frac{2}{l_{2i-1}} \boldsymbol{u}_{2i-1} \times \boldsymbol{t}_{2i}$$

$$\boldsymbol{\kappa b}_{2i}^+ = \frac{2}{l_{2i}} \boldsymbol{t}_{2i} \times \boldsymbol{u}_{2i}$$

However, this values need to be adjusted so that the static condition for rotational equilibrium ($\boldsymbol{M}^{ext} + \boldsymbol{M}^+ - \boldsymbol{M}^- = 0$) is satisfied at all time. Then, this condition will be satisfied – in particular – at the end of the solving process. To achieve this goal, we first

[9] Consequently, this model assumes that the field of tangents along the centerline is continuous and is thus unable to model cases where the centerline is not at least $\mathcal{C}^1$. In such case the beam must be considered as two parts glued together.

[10] Remark that the centerline is now approximated with a biarc in the vicinity of $\boldsymbol{x}_{2i}$. This is the reason why this model is called the "biarc model".

[11] This model offers the ability to represent discontinuities in curvature – thus in bending moment – at handle vertices as the left and right curvatures does not necessarily agree. This is quite different from the classical 3-dof element [Bar99, ABW99, DBC06] which assumes that the curvature – thus the bending moment – is $\mathcal{C}^0$ and can be evaluated at every vertices from the circumscribed osculating circle.

compute a realistic mean value ($\boldsymbol{M}_{2i}$) for the internal bending moment as :

$$\boldsymbol{M}_{2i} = \frac{1}{2}\boldsymbol{B}_{i-1}(\boldsymbol{\kappa b}_{2i}^{-} - \overline{\boldsymbol{\kappa b}}_{2i}^{-}) + \frac{1}{2}\boldsymbol{B}_{i}(\boldsymbol{\kappa b}_{2i}^{+} - \overline{\boldsymbol{\kappa b}}_{2i}^{+}) \tag{5.30}$$

To enforce the jump discontinuity in bending moment ($\boldsymbol{M}^{ext} = \boldsymbol{M}^{-} - \boldsymbol{M}^{+}$) across the handle vertex, we define the left and right bending moments at $\boldsymbol{x}_{2i}$ as :

$$\boldsymbol{M}_{2i}^{-} = \boldsymbol{M}_{2i} + \frac{1}{2}\boldsymbol{M}_{2i}^{ext} \tag{5.31a}$$

$$\boldsymbol{M}_{2i}^{+} = \boldsymbol{M}_{2i} - \frac{1}{2}\boldsymbol{M}_{2i}^{ext} \tag{5.31b}$$

Note that in the case where no external concentrated bending moment is applied to the handle vertex, the internal bending moment is continuous across the vertex.

Left/right curvatures at handle vertices

Finally, the left and right curvatures at handle vertex $\boldsymbol{x}_{2i}$ are computed back with the constitutive law :

$$\boldsymbol{\kappa b}_{2i}^{-} = \boldsymbol{B}_{i-1}^{-1}\boldsymbol{M}_{2i}^{-} + \overline{\boldsymbol{\kappa b}}_{2i}^{-} \tag{5.32a}$$

$$\boldsymbol{\kappa b}_{2i}^{+} = \boldsymbol{B}_{i}^{-1}\boldsymbol{M}_{2i}^{+} + \overline{\boldsymbol{\kappa b}}_{2i}^{+} \tag{5.32b}$$

Bending moment at ghost vertices

The internal bending moment at ghost vertices is simply given by the constitutive law as :

$$\boldsymbol{M}_{2i-1} = \boldsymbol{B}_{i-1}(\boldsymbol{\kappa b}_{2i-1} - \overline{\boldsymbol{\kappa b}}_{2i-1}) \tag{5.33a}$$

$$\boldsymbol{M}_{2i+1} = \boldsymbol{B}_{i}(\boldsymbol{\kappa b}_{2i+1} - \overline{\boldsymbol{\kappa b}}_{2i+1}) \tag{5.33b}$$

5.5.4 Discret twisting moment

We assume the twisting moment and the rate of twist to vary linearly over $]\boldsymbol{x}_{2i}, \boldsymbol{x}_{2i+2}[$. Thus, the rate of twist at mid edge is given by :

$$\tau_{i+1/2} = \frac{\Delta\theta_i}{l_i} \tag{5.34}$$

And $\theta_{i+1} - \theta_i$ is the additional twisting angle between two frames with parallel transport.

$$Q_{i+1/2} = GJ(\tau_{i+1/2} - \bar{\tau}_{i+1/2}) \tag{5.35}$$

5.5.5 Discret axial force

We assume the axial force and the axial strain to vary linearly over $]\boldsymbol{x}_{2i}, \boldsymbol{x}_{2i+2}[$. Thus, the axial strain at mid edge is given by :

$$\epsilon_{i+1/2} = \frac{l_i}{\overline{l}_i} - 1 \tag{5.36}$$

$$N_{i+1/2} = ES\epsilon_{i+1/2} \tag{5.37}$$

5.5.6 Discret shear force

Shear forces are computed from the second Kirchhoff law, considering that the inertial term is negligible.

$$\boldsymbol{F}_{i+1/2} = \boldsymbol{d}_{3,i+1/2} \times (\boldsymbol{M}'_{i+1/2} + \boldsymbol{m}_{ext,i}) + Q_{i+1/2}\boldsymbol{\kappa b}_{i+1/2} - \tau_{i+1/2}\boldsymbol{M}_{i+1/2} \tag{5.38}$$

5.5.7 Interpolation

5.6 Conclusion

Remind that the beam is subject to a distributed external force $\boldsymbol{f}_{ext}$ and a distributed external moment $\boldsymbol{m}_{ext}$.

We neglect rotational inertial effects on $\boldsymbol{d}_1$ et $\boldsymbol{d}_2$ in (**??**) and (**??**) which leads to the following shear force :

$$\boldsymbol{F}^{\perp}(s) = \boldsymbol{d}_3 \times (\boldsymbol{M}' + \boldsymbol{\Omega} \times \boldsymbol{M} + \boldsymbol{m}_{ext}) \tag{5.39}$$

$$\boldsymbol{F}^{\parallel}(s) = N\boldsymbol{d}_3 \tag{5.40}$$

We may neglect as well the last term ($\tau\boldsymbol{M}$) and get back to the shear force obtained by the variational approach.The total internal force acting on the beam is hence given by :

$$\boldsymbol{F}(s) = \boldsymbol{N}(s) + \boldsymbol{T}(s) \tag{5.41}$$

Sections are subject to the following rotational moment around the centerline :

$$\boldsymbol{\Gamma}(s) = Q' + \boldsymbol{d}_3 \cdot (\kappa\boldsymbol{b} \times \boldsymbol{M} + \boldsymbol{m}_{ext}) \tag{5.42}$$

Bibliography

[ABW99] Sigrid Adriaenssens, Michael Barnes, and Christopher Williams. A new analytic and numerical basis for the form-finding and analysis of spline and gridshell structures. In B Kumar and B H V Topping, editors, *Computing Developments in Civil and Structural Engineering*, pages 83–91. Civil-Comp Press, Edinburgh, 1999.

[Ant05] Stuart Antman. *Nonlinear problems of elasticity*. Applied mathematical sciences. Springer, New York, 2005.

[BAK13] Michael Barnes, Sigrid Adriaenssens, and Meghan Krupka. A novel torsion/bending element for dynamic relaxation modeling. *Computers & Structures*, 119:60–67, apr 2013.

[Bar99] Michael Barnes. Form Finding and Analysis of Tension Structures by Dynamic Relaxation. *International Journal of Space Structures*, 14(2):89–104, 1999.

[BEL+93] D Bernard, H Ellis, M A I O Lembo, L U Zheng, and Irwin Tobias. On the Dynamics of Rods in the Theory of Kirchhoff and Clebsch. 121:339–359, 1993.

[CBd13] Romain Casati and Florence Bertails-descoubes. Super space clothoids. In *SIGGRAPH*, 2013.

[Day65] Alister Day. An Introduction to dynamic relaxation. *The Engineer*, 1965.

[DBC06] Cyril Douthe, Olivier Baverel, and Jean-François Caron. Formfinding of a grid shell in composite materials. *Journal of the IASS*, 47:53–62, 2006.

[Dil92] Ellis Harold Dill. Kirchhoff's theory of rods. *Archive for History of Exact Sciences*, page 23, 1992.

[DKZ14] B. D'Amico, A. Kermani, and H. Zhang. Form finding and structural analysis of actively bent timber grid shells. *Engineering Structures*, 81:195–207, 2014.

[DLP13] Ye Duan, Dong Li, and P. Frank Pai. Geometrically exact physics-based modeling and computer animation of highly flexible 1D mechanical systems. *Graphical Models*, 75(2):56–68, 2013.

[dPTL+15] Lionel du Peloux, Frédéric Tayeb, Baptiste Lefevre, Olivier Baverel, and Jean-François Caron. Formulation of a 4-DoF torsion / bending element for the formfinding of elastic gridshells. In *Proceedings of the International Association for Shell and Spatial Structures*, number August, pages 1–14, Amsterdam, 2015.

[DZK16] B. D'Amico, H. Zhang, and A. Kermani. A finite-difference formulation of elastic rod for the design of actively bent structures. *Engineering Structures*, 117:518–527, 2016.

[Hoo06] P C J Hoogenboom. 7 Vlasov torsion theory. (October):1–12, 2006.

[LL09] Holger Lang and Joachim Linn. Lagrangian field theory in space-time for geometrically exact Cosserat rods. 150:21, 2009.

[MPW14] Christoph Meier, Alexander Popp, and Wolfgang A. Wall. An objective 3D large deformation finite element formulation for geometrically exact curved Kirchhoff rods. *Computer Methods in Applied Mechanics and Engineering*, 278(August):445–478, 2014.

[Neu09] S. Neukirch. *Enroulement, contact et vibrations de tiges élastiques.* PhD thesis, 2009.

[Spi08] Jonas Spillmann. *CORDE : Cosserat rod elements for the animation of interacting elastic rods.* PhD thesis, 2008.

[The07] Adrien Theetten. *Splines dynamiques géométriquement exactes : simulation haute performance et interaction.* PhD thesis, Université des Sciences et Technologies de Lille, 2007.

[Wak80] David Wakefield. *Dynamic relaxation analysis of pretensioned networks supported by compression arches.* PhD thesis, City University London, 1980.